Time Rate of Local Scour at a Circular Pile

by

William Miller Jr.[1] and D. Max Sheppard[2]

ABSTRACT

A mathematical model for the time variation of local scour depth at a singular circular pile has been developed. The scour hole shape is assumed to be that of an inverted frustum of a right circular cone with an angle equal to the angle of repose of the submerged sediment. It is assumed that the area being eroded is confined to a narrow band adjacent to the pile and that the surrounding sediment avalanches into this region so as to maintain the slope of the scour hole equal to the angle of repose. The area of erosion is further limited to an arc roughly extending from the stagnation point to the point of flow separation ($\sim \pm 90^0$ from the leading edge). Sediment transport in the area of erosion is assumed to be due to the effective shear stress in this area created by the mean and secondary flows (horseshoe vortex). The variation of effective shear stress with normalized scour depth has been established based on accurate time history scour data and a flat bed sediment transport function. The form of the sediment transport function is based on those for transport on a flat bed. As might be expected, the shape of the normalized shear stress versus normalized scour depth plots was found to depend on the same sediment, flow and structure dimensionless parameters that govern the equilibrium scour depth. This model requires the use of predictive equations for computing equilibrium scour depths for the conditions encountered in the analysis. The model was developed for clearwater conditions but can be extended to include live bed scour when sufficient data is available for model validation.

INTRODUCTION

Current practice in bridge foundation design requires that design scour depths be estimated as the ultimate (or equilibrium) scour depth for steady flow under design flow conditions. However, for many situations the duration of the peak velocity is insufficient for the scour hole to reach an equilibrium state. This is especially true in the coastal environment where the design flow conditions are usually unsteady, episodic events of relatively short duration (e.g. hurricane generated storm surge). Another factor affecting the percentage of equilibrium scour depth achieved during a design flow event is the magnitude of the design flow velocity. In the tidal plains of many coastal areas, where the terrain is very flat, design flow velocities can be relatively low and thus the rate of scour is small. In order to predict scour depths under these conditions a time dependent model that is capable of handling unsteady flows is needed.

[1] Graduate Research Assistant, Civil and Coastal Engineering Department, University of Florida, Gainesville, FL 32611, wmiller@ufl.edu.
[2] Professor of Civil and Coastal Engineering, University of Florida, Gainesville, FL 32611, sheppard@ufl.edu

MODEL DERIVATION

The model developed in this paper assumes that the geometry of the scour hole can be approximated as an inverted frustum of a right circular cone. Also, as observed by Melville (1975), Ettema (1980) and Nakagawa and Suzuki (1975), it is assumed that sediment is removed only from within a region immediately adjacent to the pier and that this area (the erosion zone) is fed by sediment avalanching down the sides of the scour hole. Following Nakagawa and Suzuki (1975), the width of the erosion zone is assumed to be constant with time and only a function of the diameter of the cylinder. Figure 1 defines the erosion zone and Figure 2 defines the volumes used in the model development and calculation.

The following relationships can be developed using the variables defined in Figures 1 and 2:

$$r_1 = \frac{D}{2} + nD, \quad r_2 = \frac{d_s}{\tan\phi}, \text{ and } \quad \Delta r = \frac{\Delta d_s}{\tan\phi}.$$

The volume of the annulus at the base of the scour hole (ΔV_1) can be calculated from

$$\Delta V_1 = \pi \Delta d_s r_1^2 - \pi \Delta d_s \left(\frac{D}{2}\right)^2 = \pi \Delta d_s nD^2 (1+n). \tag{1}$$

The volume of avalanche material ($\Delta \forall_2$) is calculated as follows

$$\Delta V_{A1} = \int_0^{d_s} \Delta A \, dy = \int_0^{d_s} \left[\pi (r+\Delta r)^2 - \pi r^2\right] dy = \int_0^{d_s} \left\{ 2\pi \left[\tfrac{1}{2} D(2n+1) + \frac{d_s}{\tan\phi} \right] \frac{\Delta d_s}{\tan\phi} + \pi \left(\frac{\Delta d_s}{\tan\phi} \right)^2 \right\} dy$$

$$\Delta V_2 = \Delta V_{A1} + \Delta V_{A2} = \pi \Delta d_s \left[D(2n+1) \frac{d_s}{\tan\phi} + \left(\frac{d_s}{\tan\phi} \right)^2 \right] + \pi \left(\frac{\Delta d_s}{\tan\phi} \right)^2 d_s + \Delta V_{A2}. \tag{2}$$

It can be shown that the small wedge shaped volume (ΔV_{A2}) beside the erosion zone annulus is a function of Δd_s^2 and Δd_s^3 and in the limit goes to zero, so that it is neglected in this calculation.

Adding Equations (1) and (2) gives the total change in volume for a given time increment, Δt. Therefore, the rate of change of volume of the scour hole is

$$\frac{\Delta \forall}{\Delta t} = \pi \frac{\Delta d_s}{\Delta t} \left[nD^2 (1+n) + D(2n+1) \frac{d_s}{\tan\phi} + \left(\frac{d_s}{\tan\phi} \right)^2 \right].$$

Or in the limit as $\Delta t \to 0$

$$\frac{d \forall}{dt} = \pi \frac{d(d_s)}{dt} \left[nD^2 (1+n) + D(2n+1) \frac{d_s}{\tan\phi} + \left(\frac{d_s}{\tan\phi} \right)^2 \right]. \tag{3}$$

Next, relate this rate of change in volume to the transport of material out of the scour hole. Defining porosity (p) as

$$p = \frac{\forall_w}{\forall_s + \forall_w} = \frac{\forall_w}{\forall},$$

the volume of sediment ($\forall_s$) removed can be related to the volume of the scour hole ($\forall$) by

$$\forall = \frac{\forall_s}{(1-p)}. \tag{4}$$

The volume rate of transport of sediment can be described by

$$\frac{d\forall_s}{dt} = Q = qw, \tag{5}$$

where Q is the rate of transport of material by volume (m^3/s), q is the rate of transport of material by volume per unit width (m^2/s) and w is the width of the area over which the sediment transport function acts. Combining Equations (4) and (5) gives

$$\frac{d\forall}{dt} = \frac{d(\forall_s/(1-p))}{dt} = \frac{d\forall_s}{dt}\frac{1}{1-p} = \frac{qw}{1-p}. \tag{6}$$

If it is assumed that the sediment is transported out of the erosion area perpendicular to the pile as shown in Figure 3, than the width in Equation (6) can be estimated by

$$w = \beta_m 2r = \beta_m 2\left(\frac{D}{2} + nD\right) = \beta_m D(2n+1),$$

where β_m is half of the perimeter of the erosion zone in radians (see Figure 1), D is the diameter of the cylinder and nD is the width of the erosion zone. Equation (6) then becomes

$$\frac{d\forall}{dt} = \frac{qD(2n+1)\beta_m}{1-p}. \tag{7}$$

Combining Equations (3) and (6) gives the relationship between the rate of change of depth of the scour hole and the sediment transport

$$\frac{qD(2n+1)\beta_m}{1-p} = \pi\frac{d(d_s)}{dt}\left[nD^2(1+n) + D(2n+1)\frac{d_s}{\tan\phi} + \left(\frac{d_s}{\tan\phi}\right)^2\right]. \tag{8}$$

Equation (8) can be non-dimesionalized with respect to length and the non-dimensional scour depth can be defined as $y = d_s/d_{se}$. Solving for dy/dt gives

$$\frac{dy}{dt} = qD(2n+1)\beta_m \Bigg/ \left\{\pi(1-p)d_{se}\left[nD^2(1+n) + D(2n+1)\frac{d_{se}y}{\tan\phi} + \left(\frac{d_{se}y}{\tan\phi}\right)^2\right]\right\}. \tag{9}$$

Note that dy/dt has dimensions of $time^{-1}$. To reduce the algebra, introduce the variable K, defined as follows:

$$K = \frac{\pi(1-p)d_{se}}{\beta_m D(2n+1)}\left[nD^2(1+n) + D(2n+1)\frac{d_{se}y}{\tan\phi} + \left(\frac{d_{se}y}{\tan\phi}\right)^2\right]. \tag{10}$$

This reduces the rate equation to the following form:

$$\frac{dy}{dt} = \frac{q}{K}. \tag{11}$$

The next step is to decide on an appropriate sediment transport relationship. Many formulas exist in the literature and it should be kept in mind that the shear stress in the erosion zone within the scour hole is highly episodic, due to the unsteady nature of the horseshoe vortex, and the flow has a strong downward component. Therefore, any formula developed for flow over a flat bed can only approximate a time mean transport in the scour hole. Though somewhat arbitrary, the choice made here was that of Engelund and Hansen (1972), who based their sediment

transport formula on an energy balance. This choice was based on both the simplicity of the formula and the use of an energy balance concept where an excess shear stress serves to mobilize the sediment which is then carried away by the near bed flow. It is hoped that such a scheme will smooth out the effects of the episodic flow. Thus, q in Equation (11) becomes

$$q = C\sqrt{\theta}\left(\theta - \theta_c\right) , \tag{12}$$

where $\theta \equiv u_*^2 / \left(sg - 1\right) gD_{50}$ is the non-dimensional bed shear stress (also known as the sediment number) and θ_c is the critical non-dimensional bed shear stress for the given sediment. The coefficient, C, is assumed to be constant with time and depth for a given set of flow conditions. This is not the constant based on depth and sediment size in the Engelund and Hansen formulation. Thus, equation (12) is not the actual bedload formula of Engelund and Hansen. The bed shear stress is actually an "effective" bed shear stress and may be thought of as the time averaged bed shear stress produced by the mean and secondary flows in the erosion area.

Combining Equations (11) and (12) results in an equation for the time rate of change of the scour depth in terms of effective bed shear stress in the erosion area and the geometry of the scour hole,

$$\frac{dy}{dt} = \frac{C\sqrt{\theta}\left(\theta - \theta_c\right)}{K} . \tag{13}$$

EFFECTIVE SHEAR STRESS BEHAVIOR

The initial value of the non-dimensional bed shear stress in the erosion zone near the pile, θ_0, can be related to the value on the flat bed upstream of the pile using the following reasoning. For scour to be initiated at the structure, the local bed shear stress must exceed the critical shear stress for the sediment. For circular piles, experiments show that the scour does not occur for values of upstream depth averaged velocity below approximately $0.45V_c$. In other words, the upstream depth averaged velocity must be approximately $0.45V_c$ in order for the velocity near the pile to be V_c and scour initiated. Assuming that the bed shear stress (τ) is proportional to the depth averaged velocity squared, we find that

$$\frac{\tau_0}{\tau_u} = \frac{U_c^2}{\left(0.45U_c^2\right)} = \frac{1}{0.45^2} \approx 4.9 ,$$

where τ_0 is the bed shear stress at the pile prior to local scour and τ_u is the upstream bed shear stress. In non-dimensional terms, $\theta_0 = 4.9\theta_u$.

The value for the constant, C, in Equation (12) can now be estimated from experimental data by applying initial conditions to Equation (13). Knowing the time history of the scour depth, dy/dt at t = 0 and K at t = 0 and y = 0 can be determined. The value for C becomes

$$C = \left.\frac{dy}{dt}\right|_0 \frac{K_0}{\sqrt{\theta_0}\left(\theta_0 - \theta_c\right)} . \tag{14}$$

Substituting this value into Equation (13) and calculating dy/dt from a known time history plot, an "effective shear stress" in the erosion area can be back calculated for each data set.

Many researchers (e.g. Sheppard et al., 1995; Ontowirjo, 1994; Melville and Sutherland, 1989) have found that equilibrium scour depths at circular piles can be adequately expressed in terms of the dimensionless quantities V/V_c, y_0/D and D/D_{50}. It is reasonable to assume that the functional dependence of the effective shear stress on scour depth will depend on these same quantities. In order to determine this functional dependence, time history scour depth data is needed from experiments where these quantities are varied; preferably, experiments where two of these groups are held constant while varying the third. The data set used in this study provides the minimal data needed for this analysis. More data is needed and is currently being acquired.

EXPERIMENTAL DATA USED IN THIS ANALYSIS

All of the experimental data used in this investigation is from a study by Sheppard et al. (2002). A number of clearwater scour experiments were conducted in a large 6.1 m wide, 6.4 m deep, 38.4 m long, flow-through type flume located in the USGS Laboratory in Turners Falls, Massachusetts. Three different circular piles (with diameters 0.915 m, 0.305 m, and 0.114 m), three different sediment grain sizes (D_{50} = 0.22 mm, 0.80 mm and 2.9 mm) and a range of water depths were investigated.

The flow parameters monitored were flow discharge (indirectly), velocity, and water depth and temperature. The scour depth was monitored with video cameras inside the piles and with arrays of acoustic transponders attached to the exterior of the piles, just below the water surface. This system provided scour depth measurements at 12 locations along three radial lines throughout the experiments. The tests lasted from 41 hours to 650 hours and were such that near equilibrium scour depth conditions were achieved. Equilibrium scour depths were estimated by extrapolating the curve fit Equation (15), first used by Bertoldi and Jones (1998) and found by Sheppard et al. (2002) to adequately fit their data.

$$d_s(t) = a\left[1 - \frac{1}{(1+abt)}\right] + c\left[1 - \frac{1}{(1+cdt)}\right], \tag{15}$$

where a, b, c, d are constant coefficients determined from the data and t is time. Table 1 summarizes the results.

Experiment numbers 7, 8, 9 and 10 (with D_{50} = 2.9 mm sediment and D = 0.914 m diameter pile) give the best information about the effects of the aspect ratio, y_0/D, on the shear stress versus scour depth relationship. D/D_{50} is the same and V/V_c is nearly constant (0.78 – 0.89) for these experiments. Normalized excess shear stress [shear stress in excess of the critical value, $(\theta-\theta_c)$] versus normalized scour depth plots for Experiments 7-10 are presented in Figure 4. The excess shear stress is normalized by the maximum excess shear stress, $(\theta_p-\theta_c)$, where θ_p is the peak shear stress, and the scour depth is normalized by the equilibrium scour depth, d_{se}.

Figure 5 compares the results from Experiments 1 and 6 and illustrates the case where the aspect and velocity ratios are nearly constant and the normalized sediment size varies. There were no tests in this data set with both D/D_{50} and y_0/D constant and variable V/V_c. The closest approximation of constant D/D_{50} and y_0/D and variable V/V_c is between Experiments 7 and 11

(Figure 4, plot 1 and Figure 6, plot 1, respectively). Though an effect from the aspect ratio difference is expected, since the shear decreases from Experiment 7 to Experiment 11 while the aspect ratio increases (an effect opposite to the trend of Figure 4), it can be assumed that this is the result of the reduction in V/V_c. Also included in Figure 6 is a plot of Experiment 14 which illustrates the effect of large values of D/D_{50} and V/V_c, with an average value for the aspect ratio.

Table 1, Summary of Experiments

exp	D (m)	D_{50} mm)	y_0 (m)	V (m/s)	V/V_c	y_0/D	D/D_{50}	d_{se}/D
1	0.114	0.22	1.19	0.29	0.89	10.44	518	1.38
2	0.305	0.22	1.19	0.31	0.96	3.90	1386	1.34
3	0.915	0.80	1.27	0.40	0.85	1.39	1143	1.20
4	0.915	0.80	0.87	0.39	0.84	0.95	1143	1.04
5	0.305	0.80	1.27	0.39	0.82	4.16	381	1.41
6	0.114	0.80	1.27	0.41	0.87	11.14	143	1.58
7	0.915	2.90	1.22	0.76	0.89	1.33	315	1.51
8	0.915	2.90	0.56	0.65	0.85	0.61	315	1.20
9	0.915	2.90	0.29	0.57	0.83	0.32	315	1.05
10	0.915	2.90	0.17	0.50	0.78	0.19	315	0.79
11	0.915	2.90	1.90	0.70	0.75	2.08	315	1.28
12	0.305	0.22	1.22	0.40	1.23	4.00	1386	1.28
13	0.305	0.22	0.18	0.30	1.10	0.59	1386	0.95
14	0.915	0.22	1.81	0.30	0.95	1.98	4155	1.06

The general behavior of the shear stress with scour depth obtained by this method is consistent with descriptions of local scour processes published in the literature and observed by the authors of this paper. Melville (1975) and Ettema (1980) described three phases of scour as an "initial phase" where the scour hole forms from the flat-bed condition, followed by the "principle erosion phase" where the horseshoe vortex grows rapidly in size and strength and settles into the scour hole. Finally, the "equilibrium phase" occurs where the flow is no longer able to remove sediment. Nakagawa and Suzuki (1975) gave a similar description with four stages: "1) scour near the side of the pier caused by tractive force of the main flow, 2) scour near the leading edge generated by a horseshoe vortex, 3) scour developed by the stable vortex flowing along the pier, and 4) reduction in scour rate due to decrease in transport capacity in the hole."

The observed size and intensity of the horseshoe vortex prior to local scour is, in general, less than it is once the scour hole is formed. Flow separation at the edge of the scour hole feeds energy to the vortex and increases both its size and strength. It is logical that the shear stress will increase initially with scour depth and then at some depth start to decrease. Ultimately, it must reach a value near the critical shear stress where the removal of sediment stops. It also appears that the maximum obtainable size and strength of the horseshoe vortex is primarily a function of the pile diameter and the mean flow velocity. The dependence on pile diameter is believed to diminish with increased pile diameter (Sheppard et al., 2002). The rather abrupt change in the slope of the shear stress versus scour depth when the depth reaches about half the equilibrium value is thought to be the point when the horseshoe vortex is submerged in the scour hole. The rate of shear stress decrease with scour depth is much less from this point to the equilibrium depth.

The combined effects of the aspect ratio (normalized water depth, y_0/D) and normalized velocity (V/V_c) on these processes can be seen in the sequence of plots in Figure 4. As the water depth decreases, for a given pile size, the interference between the surface vortex (surface roller) and the horseshoe vortex increases. This attenuates the strength of the horseshoe vortex and retards its ability to increase the shear stress as the scour hole initially progresses. This also causes the shear stress to be reduced to near the critical value at about half of the equilibrium depth. In the limiting cases of shallow water the rate of scour is very slow for the latter half of the depth. An additional effect reducing the shear stress is the reduction in normalized velocity in this sequence of plots. More data is needed to separate the effects of aspect ratio and velocity.

The effects of normalized sediment size, D/D_{50} can be seen in the plots in Figure 5 and the first plot of Figure 4 (Experiment 7). As the diameter of the pile is decreased (or the sediment size increased) the shear stress remains above the initial value for a greater portion of the scour hole development and the flatter portion of the curve becomes almost non existent. Possible explanations for this behavior are given from the standpoint of changing pile size while keeping the sediment size constant and vice versa. If the sediment diameter is fixed and the pile diameter allowed to decrease (thus decreasing the values for D/D_{50}), as in going from Experiment 14 to 1 to 7 to 6, the size of the horseshoe vortex in comparison with the pile diameter increases. Thus a greater proportion of the scour hole is achieved before the vortex is submerged. If the pile diameter is held constant and the sediment size is allowed to increase (thus decreasing the values for D/D_{50}), the velocity must increase in order for V/V_c to remain constant. With the increased velocity there is more energy available in the mean flow to feed the vortex and thus the shear stress remains above the initial value for a greater proportion on the scour hole.

The data set used in this study is much less suitable for analyzing the effects of normalized velocity, V/V_c on the shear stress versus scour depth relationship. There are no two experiments where both y_0/D and D/D_{50} are held constant while varying the values of V/V_c. There are, however, experiments with different values of V/V_c in which information for the V/V_c dependency can be extracted if the above described effects of y_0/D and D/D_{50} are taken into consideration. In some cases, the effects of y_0/D and D/D_{50} can even be assumed to have reached a limit (i.e. conditions are such that the dependency on y_0/D and D/D50 is minimal). More data is being obtained to improve and verify the relationships developed and presented in this paper.

In order to solve Equation (13) for a given situation the above described relationships must be expressed analytically. The shear stress – scour depth relationship was divided into three segments. The initial segment can be approximated by a parabola with its vertex at the peak of the curve and its $y = 0$ intersection at $\theta = \theta_0$. The second segment (from the peak to the point of sharp change in slope) can likewise be represented by a second parabola with its vertex also at the peak and going through the point where the slope of the curve changes abruptly (called the peak point with $y = y_b$ and $\theta = \theta_b$). Finally, a straight line can be used to approximate the third segment. The general equations for these segments are as follows:

$$0 \le y \le y_p, \quad \theta = \theta_p - a_1\left(y - y_p\right), \text{ where } a_1 = \frac{\theta_p - \theta_0}{y_p^2}, \tag{16}$$

and y_p is the location of the peak. The second parabola can be expressed as

$$y_p \le y \le y_b, \quad \theta = \theta_p - a_2\left(y - y_p\right), \text{ where } a_2 = \frac{\theta_p - \theta_b}{\left(y_b - y_p\right)^2}. \tag{17}$$

The final straight line segment can be expressed by the following equation:

$$y_b \le y \le 1, \quad \theta = \theta_c + m_2\left(y - 1\right). \tag{18}$$

Empirical relationships for $\left.\frac{dy}{dt}\right|_{t=0}$, θ_p, y_p, y_b, and m_2 were obtained from the data set and are given in the following equations:

$$\left.\frac{dy}{dt}\right|_0 = 0.11\left(\frac{V}{y_0}\right)\tanh\left(1.5\frac{y_0}{D}\right)\left(2.8\frac{V}{V_c} - 1\right)\left[1 + 14\exp\left(-\frac{D/D_{50}}{1200}\right)\right], \tag{19}$$

where V is in m/s and D in m,

$$\frac{\theta_p}{\theta_c} = 6.5\left(\frac{y_0}{D}\right)^{0.07}\left(\frac{V}{V_c}\right)^2\left(\frac{D}{D_{50}}\right)^{-0.03}, \tag{20}$$

$$y_p = 0.4 - 0.15\left(\frac{y_0}{D}\right)^{-0.15}\left(\frac{V}{V_c}\right)^{-0.1}\left(\frac{D}{D_{50}}\right)^{0.1}. \tag{21}$$

If the quantity $\left(\frac{y_0}{D}\right)\left(\frac{V}{V_c}\right)^2\left(\frac{D}{D_{50}}\right)^{-1.5}$ is less than 3 x 10^{-5}, then $y_p = 0$, and $\frac{\theta_p}{\theta_0} = 1$.

$$y_b = 2y_p + 0.35\left(1 - 2y_p\right), \tag{22}$$

and

$$m_2 = -0.045\left(\frac{y_0}{D}\right)^{0.7}\left(\frac{V}{V_c}\right)^{7.1}\left(\frac{D}{D_{50}}\right)^{0.11}. \tag{23}$$

Note that Equation (19) has dimensions of time^{-1} (specifically, hours^{-1}) while Equations (20) through (23) are non-dimensional. Figure 7 shows three shear stress curves calculated with Equations (16) through (18) and (20) through (23) plotted against the back-calculated shear stress curves. The results are reasonable considering the extent of the data and the approximate nature of the curve fits.

Using these relationships, Equation (13) was solved for the conditions of the experimental data using a simple fourth order Runga-Kutta technique. Predicted, measured and curve fit of the measured scour depth time history plots for four of the experiments are given in Figures 8 and 9. The first plot in Figure 8 is the prediction with the least error and the second is the prediction with the greatest error. The plots in Figure 9 are for experimental data sets with average error. Once again reasonable accuracy was achieved.

Next a hypothetical prototype scale situation was examined. A 10 m diameter circular dolphin located in cohesionless, uniform diameter sand (D_{50}= 0.3 mm) in a water depth of 10 m is subjected to a steady, depth averaged flow velocity of 0.4 m/s (V/V_c = 1). Sheppard's Equation (Sheppard et al., 2002) was used to compute an equilibrium scour depth of 4.2 m. The computed

scour depth as a function of time is shown in Figure 10. The time required to reach 50% and 90% of the equilibrium scour depth is approximately 13 days and 124 days, respectively. This is only a hypothetical problem for which there is no measured data but the results appear to be reasonable based on the authors' experience with prototype structures.

CONCLUSIONS

A method for estimating the rate at which local scour depths occur is badly needed by both researchers and practicing engineers. Attempts to produce either an empirical or computational model for this purpose have been hampered by the complexity and unsteady nature of the flow and sediment transport processes involved. Any practical attempt to analyze the time dependency of scour depths must, by necessity, work with time averaged and "effective" quantities such as shear stress. The mathematical model developed as part of the work reported here is for the local scour at a single circular pile under clearwater scour flow conditions. The model utilizes experimental data from a study by Sheppard et al. (2002) where time histories of scour depths were measured for a range of pile and sediment sizes and water depths and flow velocities.

The resulting model does a reasonable job of predicting the time histories of the experiments on which it is based, as would be expected. This does, however, show that the relationships developed for the dependency of the effective shear stress versus scour depth on the structure, sediment and flow parameters are close to those displayed by this data set. In addition, the results of the hypothetical prototype scale example seem reasonable and are consistent with what the authors have observed in their field studies. As more laboratory data is available the model can be fine tuned and improved.

The next step is to extend the model to live bed scour conditions. Good time history data for live bed scour tests is difficult to obtain and to interpret. Adding the influx of sediment to the scour hole in the model will be easy. The more difficult part will be in obtaining accurate effective shear stress versus scour depth information.

ACKNOWLEDGEMENTS

The research reported here was conducted under the sponsorship of the Florida Department of Transportation.

NOTATION

a_1	directrix (x 4) for the initial shear stress curve parabolic approximation
a_2	directrix (x 4) for the second shear stress curve parabolic approximation
D	pile/cylinder diameter
C	transport function coefficient
D_{50}	median sediment diameter
d_s	instantaneous scour depth
d_{se}	equilibrium scour depth
Δd_s	change in depth of scour in time Δt

m_2	slope for the final shear stress curve linear approximation
n	width of the entrainment zone as a fraction of the pier diameter
p	sediment porosity
Q	the rate of transport of material by volume (m^3/s)
q	the rate of transport of material by volume per unit width
sg	Sediment specific gravity (ρ_s/ρ)
V	depth averaged upstream flow velocity
V_0	initial depth averaged flow velocity at the pile required to initiate scouring
V_c	depth averaged critical velocity
$\forall$	scour hole volume
$\forall_s$	volume of sediment solids
$\forall_w$	volume of water
w	the width of the area over which the sediment transport function acts
y	non-dimensional instantaneous scour depth ($y = d_s/d_{se}$)
y_0	upstream water depth
y_p	non-dimensional instantaneous scour depth at which the shear stress peak occurs
y_b	scour depth at which the slope of the shear stress curve changes abruptly ("break")
dy/dt	time rate of scour in units of $hours^{-1}$
$dy/dt\|_0$	initial time rate of scour in units of $hours^{-1}$
β_m	half of the perimeter of the erosion zone in radians
ϕ	sediment angle of repose
θ	non-dimensional bed shear stress or sediment number, $\theta = u_*^2/(sg-1)gd_{50}$
θ_0	initial non-dimensional shear stress at the pile required to initiate scouring
θ_c	critical non-dimensional shear stress
θ_p	peak non-dimensional shear stress
θ_b	shear stress value at which the slope of the shear stress curve changes abruptly
θ_u	upstream non-dimensional shear stress
ρ	density of water
ρ_s	density of sediment particle
τ	bed shear stress, $\tau = \rho u_*^2$
τ_0	initial bed shear stress at the pile required to initiate scouring
τ_c	critical bed shear stress
τ_u	upstream non-dimensional shear stress

REFERENCES

1. Bertoldi, D.A. and Jones, J.S., 1998, " Time to Scour Experiments as an Indirect Measure of Stream Power around Bridge Piers, Proc. International Water Resources Engineering Conf, Memphis, Tenn, Aug 1998, pp. 264-269.
2. Engelund, F. and Hansen, E., 1972, "A Monograph on Sediment Transport in Alluvial Streams," Technical Press, Copenhagen.
3. Ettema, R., 1980, “Scour at Bridge Piers.” University of Auckland, School of Engineering, Auckland, New Zealand, Rep. No. 216.

4. Melville, B.W., 1975, “Local Scour at Bridge Sites.” University of Auckland, School of Engineering, Auckland, New Zealand, Rep. No. 117.
5. Melville, B.W. and Sutherland, A.J., 1989, “Design Method for Local Scour at Bridge Piers.” Journal of Hydraulic Engineering, Vol. 114, No. 10, 1210-1226, American Society of Civil Engineers, Reston, Virginia, USA.
6. Melville, B.W. and Chiew, Yee-Meng, 1999, "Time Scale for Local Scour at Bridge Piers", Journal of Hydraulic Engineering, Vol. 125, No. 1, pp. 59-65, American Society of Civil Engineers, Reston, Virginia, USA.
7. Nakagawa, H. and Suzuki, K., 1975, “An Application of Stochastic Model of Sediment Motion to Local Scour Around a Bridge Pier.” Proc. 16th IAHR Congress, Sao Paulo, Brazil, Vol. 2, pp 228-235.
8. Ontowirjo, B. 1994. "Prediction of Scour Near Single Piles in Steady Currents." Master's Thesis, UFL/COEL-94/001, Coastal and Oceanographic Engineering Department, University of Florida, Gainesville, FL.
9. Sheppard, D.M., Zhao, G., and Ontowirjo, B. 1995. “Local scour near single piles in steady currents.” ASCE Conference Proceedings: The First International Conference on Water Resources Engineering, San Antonio, TX.
10. Sheppard, D. M., 2002, “Equilibrium Local Scour Depth Prediction Under Clearwater Scour Conditions”, In Preparation, to be submitted to ASCE, J. Hydraulic Engineering,.

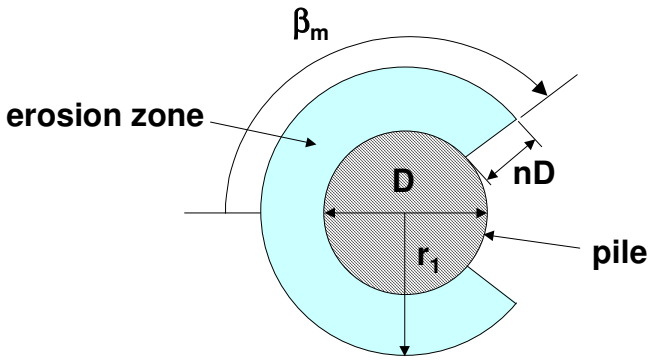

Figure 1. Definition sketch of erosion zone..

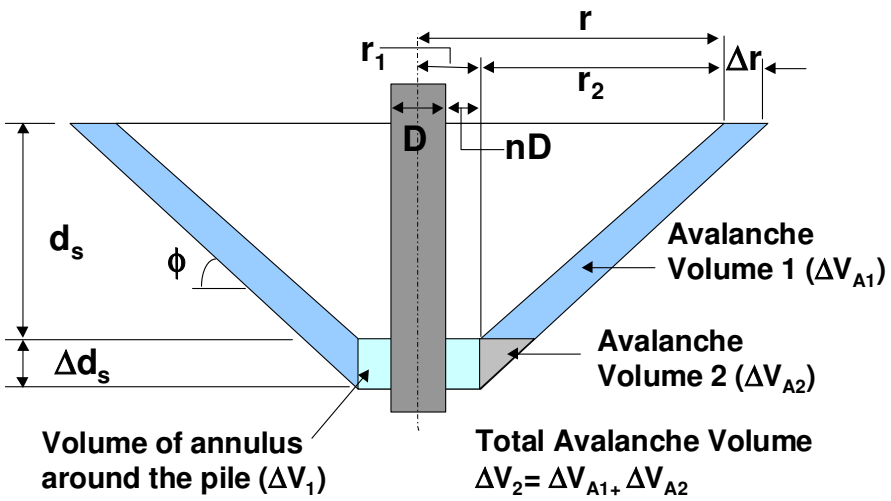

Figure 2. Definition sketch of scour hole..

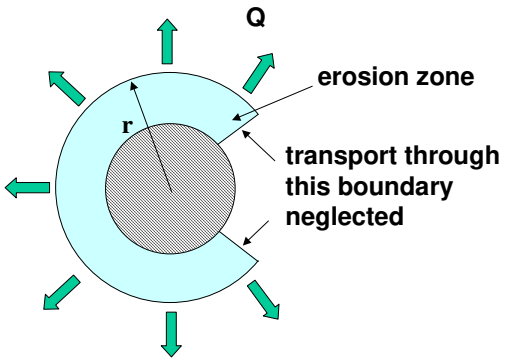

Figure 3. Diagram showing sediment transport out of the erosion zone.

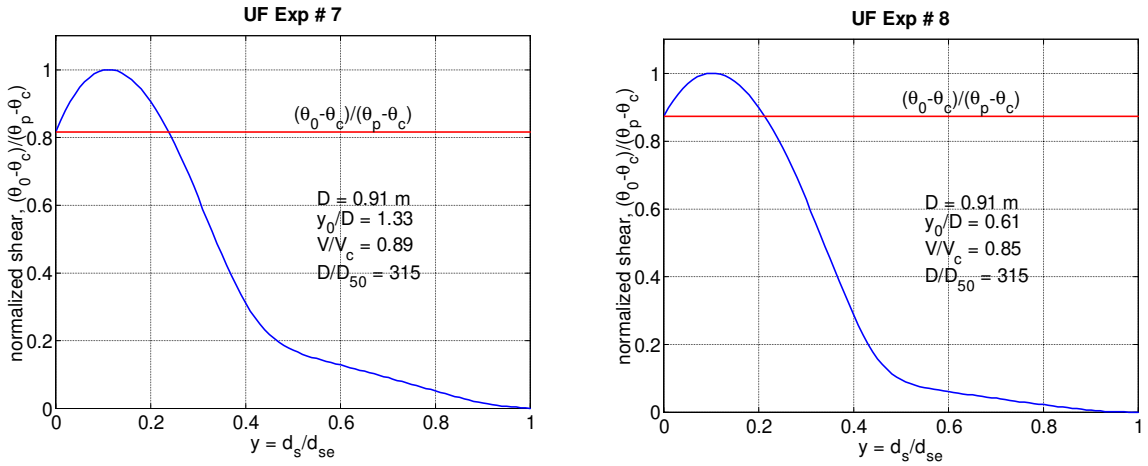

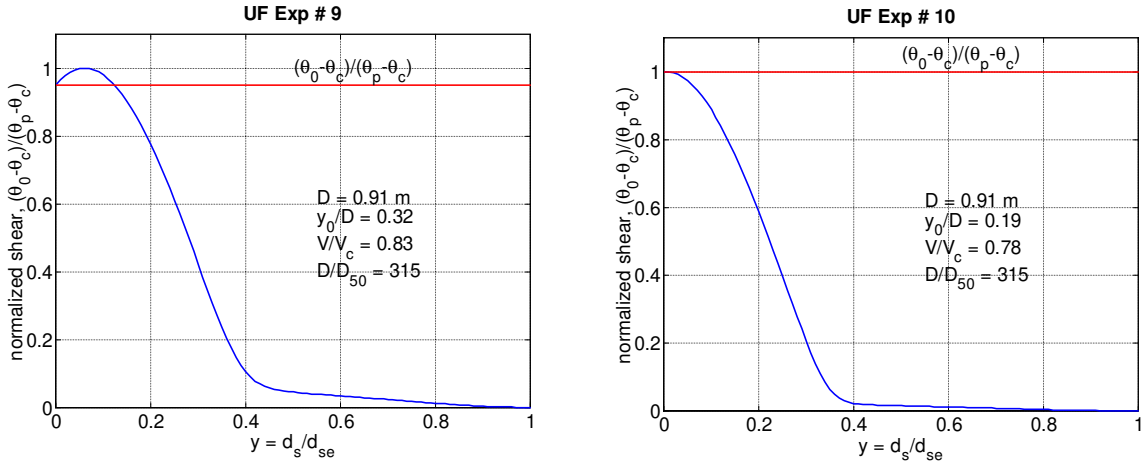

Figure 4. Effects of aspect ratio and velocity ratio on effective (back-calculated) shear stress vs. scour depth.

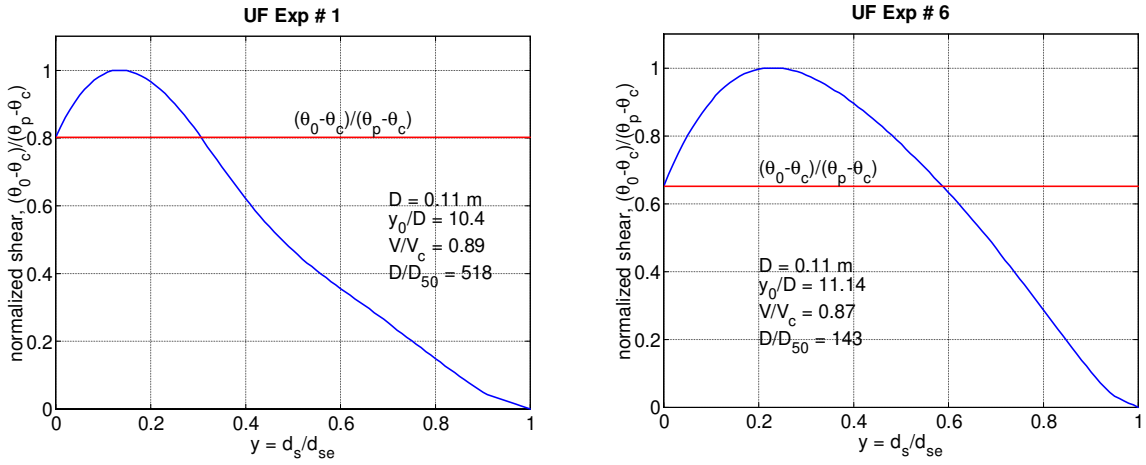

Figure 5. Effective (back-calculated) shear stress vs. scour depth for experiments 1 and 6.

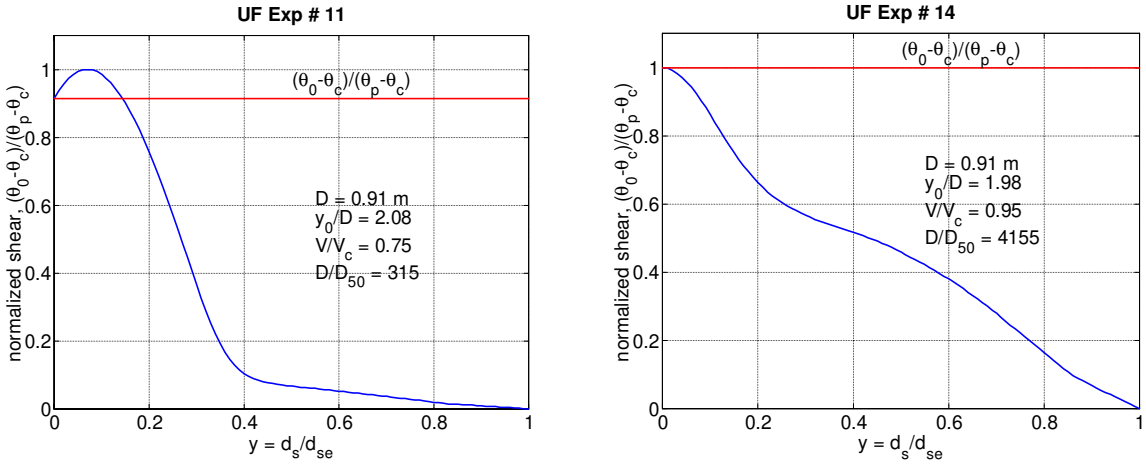

Figure 6. Effective (back-calculated) shear stress vs. scour depth for experiments 11 and 14.

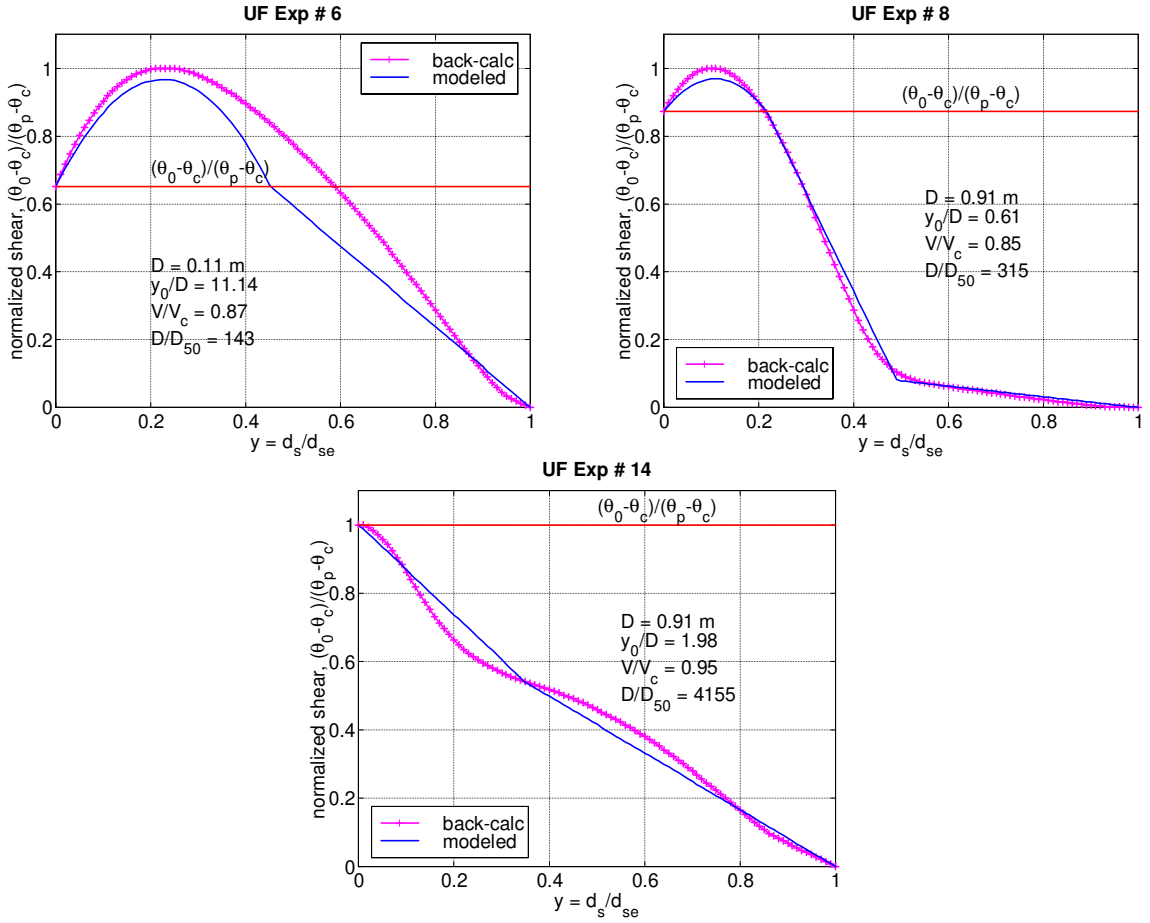

Figure 7. Modeled and back-calculated normalized shear stress, $(\theta-\theta_c)/(\theta_p-\theta_c)$ vs. Scour Depth.

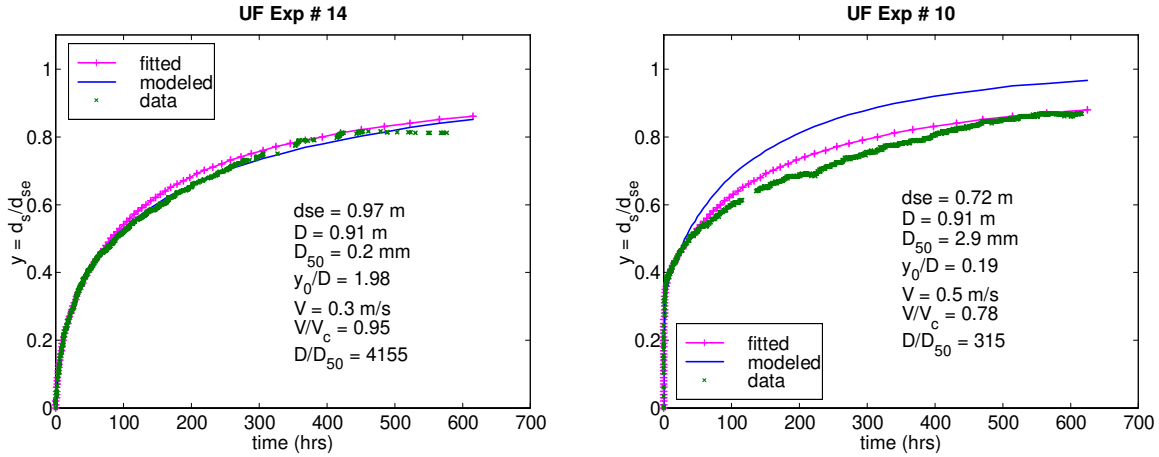

Figure 8. Fitted, modeled and measured normalized scour depth versus time for experiments 14 (least error) and 10 (greatest error).

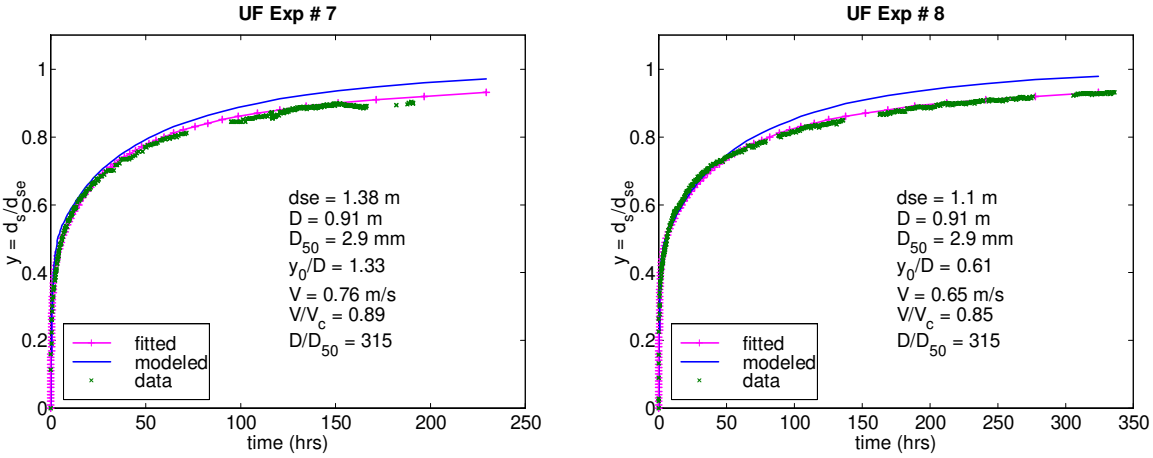

Figure 9. Fitted, modeled and measured normalized scour depth versus time for experiments 7 and 8 (average error).

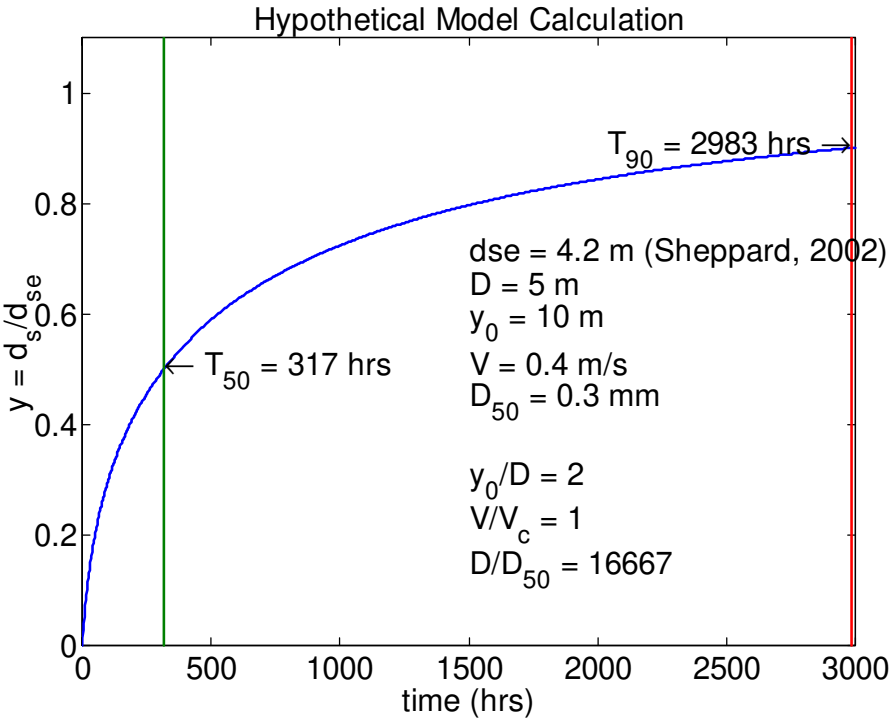

Figure 10. Computed scour depth versus time for a hypothetical prototype structure.